

Normal-state magnetic susceptibility in a bilayer cuprate

W. C. Wu,¹ B. W. Statt,² Ya-Wei Hsueh,² and J. P. Carbotte¹

¹*Department of Physics and Astronomy, McMaster University, Hamilton, Ontario, Canada L8S 4M1*

²*Department of Physics, University of Toronto, Toronto, Ontario, Canada M5S 1A7*

(July 6, 2017)

The magnetic susceptibility of high- T_c superconductors is investigated in the normal state using a coupled bilayer model. While this model describes in a natural way the normal-state pseudogaps seen in c -axis optical conductivity on underdoped samples, it predicts a weakly increasing susceptibility with decreasing temperature and cannot explain the magnetic pseudogaps exhibited in NMR measurements. Our result, together with some experimental evidence suggest that the mechanism governing the c -axis optical pseudogap is different from that for the a - b plane magnetic pseudogap.

PACS numbers: 74.80.Dm, 74.25.Jb, 74.72.-h, 76.60.-k

Normal-state pseudogaps of underdoped samples have been one of the important subjects in the study of high- T_c cuprates in the past few years [1]. Experimentally strong decrease of NMR Knight shift and spin-lattice relaxation rate with decreasing temperature has been observed in various normal-state underdoped samples below some cross over temperature T^* [2–6]. These decreases have often been considered in terms of the opening of a “spin gap” due to the antiferromagnetic (AF) spin fluctuations [7–9] or, alternatively, the notion of “preformed Cooper pairs” in the case of significant order parameter phase fluctuations [10]. Measurements on dc resistivity for underdoped samples also reveal that the in-plane resistivity $\rho_{ab}(T)$ deviates from a linear in temperature behavior at some temperature consistent with the crossover temperatures T^* in NMR experiments [11]. On the other hand, the c -axis optical conductivity $\sigma_c(\omega)$ [12–15] exhibits a striking gap-like depression at low frequency and the c -axis resistivity $\rho_c(T)$ displays a upturn semiconducting feature [11] in the normal-state underdoped samples, characteristic of the formation of some kinds of gap.

A central question in the study of pseudogaps is – are the pseudogaps seen in the c -axis optical conductivity related *at all* to the magnetic pseudogaps seen in NMR experiments? Or, could there be two different mechanisms? While there is currently no consensus on this point, we begin by comparing first some of the properties of these two pseudogaps seen in experiments. Consider the magnitude and anisotropy of these two pseudogaps: (i) *Magnitude* – Although one does not measure the magnetic pseudogap directly, an analysis done by Williams *et al.* [16] of Knight-shift data based on quasiparticle excitation spectrum given by $E_{\mathbf{k}} = [\epsilon_{\mathbf{k}}^2 + \Delta_{\mathbf{k}}^2]^{1/2}$ where $\Delta_{\mathbf{k}}$ is the normal-state pseudogap shows that the magnitude of magnetic pseudogap is strongly dependent on doping or carrier density (larger gap with lower doping) and scales with the crossover temperature T^* . In contrast, the c -axis optical conductivity measured by Homes *et al.* [13] on $\text{YB}_2\text{C}_3\text{O}_{6+x}$ (YBCO) at different doping x indicates that the frequency ranges where conductivity is suppressed (direct measurement for the size of the gap) are almost independent of doping. Moreover, a compari-

son [6] of YBCO and $\text{Pb}_2\text{Sr}_2(\text{Y,Ca})\text{Cu}_3\text{O}_{8+\delta}$ (PSYCCO) data gives that the optical pseudogap does not scale with T^* . (ii) *Anisotropy* – NMR [16] experiments reveal that the magnetic pseudogap has d -wave like anisotropy (consistent with the angular resolved photoemission spectroscopy (ARPES) [17] result), while the *flat* spectral weight seen within the pseudogap region in c -axis optical data implies that the optical pseudogap is isotropic (s -wave like). The above comparison seems to suggest that the magnetic pseudogap is intimately connected to the superconducting gap and reflects the pairing mechanism, while the optical pseudogap is due to a different mechanism.

Recently Atkinson and Carbotte [18] and with Wu [19,20] have used a coupled bilayer model to calculate various c -axis properties of the high T_c cuprates. Within this model, a minimum energy difference Δ between two non-degenerate bands (associated with two layers coupled by a single-particle hopping t_{\perp}) is introduced. This band gap Δ – turns out to be the pseudogap seen in the c -axis optical conductivity – and gives the suppression of the joint density of states in the interband transitions. The key feature of this coupled bilayer model is that the c -axis optical conductivity can be generally separated into intraband (proportional to t_{\perp}^4) and interband (proportional to t_{\perp}^2) parts. Therefore, when t_{\perp} is small which is the condition appropriate to the underdoped regime [21], interband contribution dominates over the usual intraband contribution and, as a result, the pseudogap is visible (non-Drude like behavior). In contrast in the larger t_{\perp} optimally-doped or overdoped regime, intraband dominates and one retains the more usual no-pseudogap Drude-like behavior.

It is shown in Refs. [18,20] that the coupled bilayer model explains in a natural way the pseudogap seen in the c -axis optical conductivity for underdoped, and gives an explanation of why it is not seen in optimally-doped or overdoped samples (see Fig. 1). Both temperature and frequency dependence of the entire spectrum seen in experiments [12,13] are well described by this model. It is thus not surprisingly that the semiconductor-like upturn feature at low temperature seen in the c -axis dc resistivity is also understood in this model [20]. Since this

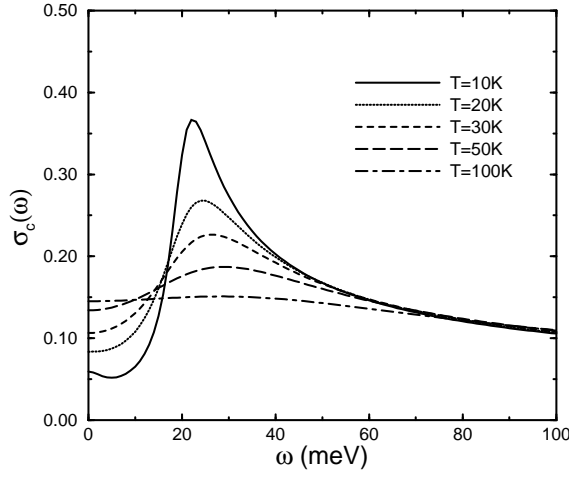


FIG. 1. Normal-state c -axis conductivity as a function of photon energy for a plane-chain bilayer at different temperatures with a small $t_{\perp} = 2\text{meV}$. The minimum energy difference between the two bands for a given \mathbf{k} in the first 2D Brillouin zone is $\Delta = 20\text{meV}$ (taken from Fig. 1 in Ref. [20]).

model emphasizes the band structure correlation arising from two non-degenerate coupled layers, a simple test can be immediately done for the single-layer $\text{La}_{2-x}\text{Sr}_x\text{CuO}_4$ (LSCO) which is found by Basov *et al.* [22] to exhibit no pseudogap in the c -axis optical conductivity or a very weak pseudogap with large energy scale $\sim 0.1\text{eV}$ by Uchida *et al.* [23]. The latter case accompanied with a semiconducting upturn feature of $\rho_c(T)$ [24] strongly suggests that while there is only one conducting layer, in practice there are *two* bands separated by a large energy difference $\Delta \sim 0.1\text{eV}$ in LSCO. We note that in this case Startseva *et al.* [25] find a strong in-plane pseudogap with smaller energy scale indicating no correlation between in-plane and out-of-plane energy scale for the pseudogap.

In the following, we use the bilayer model to calculate the magnetic susceptibility. We consider the spin raising (+) and lowering (−) operators for layer i ($i=1,2$) defined by $\sigma_{i,\mathbf{q}}^+ = \sum_{\mathbf{k}} c_{i,\mathbf{k}+\mathbf{q},\uparrow}^\dagger c_{i,\mathbf{k},\downarrow}$ and $\sigma_{i,\mathbf{q}}^- = \sum_{\mathbf{k}} c_{i,\mathbf{k}+\mathbf{q},\downarrow}^\dagger c_{i,\mathbf{k},\uparrow}$. The *transverse* (parallel to a - b plane) magnetic susceptibility χ_{ij} which we shall concentrate on, is then given by [26]

$$\chi_{ij}(\mathbf{q}, i\omega_n) = 2\mu_e^2 \int_0^\beta d\tau e^{i\omega_n \tau} \langle T_\tau \sigma_{i,\mathbf{q}}^-(\tau) \sigma_{j,-\mathbf{q}}^+(0) \rangle, \quad (1)$$

where μ_e is the Bohr magneton, χ_{11}, χ_{22} denote the in-plane spin correlation, and χ_{12}, χ_{21} denote the out-of-plane (or cross) spin correlation. Due to its local nature, an NMR experiment is able to study the spin susceptibility $\chi_{ij}(\mathbf{q}, \omega)$ individually. For example, the Knight shift (K_s) for an atom in layer i is directly proportional to the real part of the planar spin susceptibility, $K_s(T) \sim \chi'_{ii}(\mathbf{q} = 0, \omega = 0)$ and the spin-lattice relaxation rate (per temperature unit) is related

to imaginary-part susceptibility over a weighted sum, $(1/T_1 T)_i \sim \sum_{\mathbf{q}} |A(\mathbf{q})|^2 \chi''_{ii}(\mathbf{q}, \omega \simeq 0)/\omega$. While, the information contained in the cross spin susceptibility χ_{12} can be probed by a spin echo double resonance (SEDOR) experiment (see, for example, Ref. [27]).

In terms of a free electron system, the susceptibility (1) can be reduced to

$$\chi_{ij}(\mathbf{q}, i\omega_n) = -2\mu_e^2 \sum_{\mathbf{k}} \frac{1}{\beta} \sum_{\nu_n} \text{Tr}[G_0(\mathbf{k}, i\nu_n) \gamma_i G_0(\mathbf{k} + \mathbf{q}, i\nu_n - i\omega_n) \gamma_j], \quad (2)$$

tracing over the two bands, where $\gamma_1 = \begin{bmatrix} 1 & 0 \\ 0 & 0 \end{bmatrix}$ and $\gamma_2 = \begin{bmatrix} 0 & 0 \\ 0 & 1 \end{bmatrix}$ are the vertices and

$$G_0^{-1}(\mathbf{k}, i\nu_n) = \begin{bmatrix} i\nu_n - \xi_1(\mathbf{k}) & -t(k_z) \\ -t(k_z) & i\nu_n - \xi_2(\mathbf{k}) \end{bmatrix} \quad (3)$$

is the Green's function matrix. The parameter ξ_i is the band structure for isolated layer i and t is the coupling between the two layers. Considering only the $\mathbf{q} \rightarrow 0$ case, the trace operator in (2) enables one to calculate χ_{ij} in a convenient frame in which the Green's function matrix is diagonal. Consequently,

$$\chi_{ij}(\mathbf{q} = 0, i\omega_n) = -2\mu_e^2 \sum_{\mathbf{k}} \frac{1}{\beta} \sum_{\nu_n} \text{Tr}[\hat{G}_0(\mathbf{k}, i\nu_n) \hat{\gamma}_i \hat{G}_0(\mathbf{k}, i\nu_n - i\omega_n) \hat{\gamma}_j], \quad (4)$$

where

$$\hat{G}_0^{-1}(\mathbf{k}, i\nu_n) = \begin{bmatrix} i\nu_n - \epsilon_+ + i\Gamma_+ \text{sgn}(\nu_n) & 0 \\ 0 & i\nu_n - \epsilon_- + i\Gamma_- \text{sgn}(\nu_n) \end{bmatrix}, \quad (5)$$

with Γ_{\pm} introduced as the total scattering rate in band \pm . The two renormalized bands are

$$\epsilon_{\pm} = \frac{\xi_1 + \xi_2}{2} \pm \sqrt{\left(\frac{\xi_1 - \xi_2}{2}\right)^2 + |t|^2} \quad (6)$$

and the rotated vertices are

$$\hat{\gamma}_1 = \begin{bmatrix} \alpha_{11} & \alpha_{12} \\ \alpha_{12} & \alpha_{22} \end{bmatrix}; \quad \hat{\gamma}_2 = \begin{bmatrix} \alpha_{22} & -\alpha_{12} \\ -\alpha_{12} & \alpha_{11} \end{bmatrix}, \quad (7)$$

where $\alpha_{11} \equiv (\xi_1 - \epsilon_-)/(\epsilon_+ - \epsilon_-)$, $\alpha_{22} \equiv (\epsilon_+ - \xi_1)/(\epsilon_+ - \epsilon_-)$, and $\alpha_{12} \equiv |t|/(\epsilon_+ - \epsilon_-)$. Substituting (5) and (7) into (4), we obtain

$$\begin{aligned} \chi_{11}(i\omega_n) &= -2\mu_e^2 \sum_{\mathbf{k}} \frac{1}{\beta} \sum_{\nu_n} \left[\left(\alpha_{11}^2 G_{11} G'_{11} + \alpha_{22}^2 G_{22} G'_{22} \right) \right. \\ &\quad \left. + \alpha_{12}^2 \left(G_{11} G'_{22} + G_{22} G'_{11} \right) \right], \\ \chi_{22}(i\omega_n) &= -2\mu_e^2 \sum_{\mathbf{k}} \frac{1}{\beta} \sum_{\nu_n} \left[\left(\alpha_{22}^2 G_{11} G'_{11} + \alpha_{11}^2 G_{22} G'_{22} \right) \right. \\ &\quad \left. + \alpha_{12}^2 \left(G_{11} G'_{22} + G_{22} G'_{11} \right) \right], \end{aligned}$$

$$\begin{aligned}
& + \alpha_{12}^2 (G_{11}G'_{22} + G_{22}G'_{11}) \Big], \\
\chi_{12}(i\omega_n) = \chi_{21}(i\omega_n) = & -2\mu_e^2 \sum_{\mathbf{k}} \frac{1}{\beta} \sum_{\nu_n} \left[\alpha_{11}\alpha_{22} (G_{11}G'_{11} \right. \\
& \left. + G_{22}G'_{22}) - \alpha_{12}^2 (G_{11}G'_{22} + G_{22}G'_{11}) \right], \quad (8)
\end{aligned}$$

where $G_{ii} \equiv G_{ii}(\mathbf{k}, i\nu_n)$ and $G'_{ii} \equiv G_{ii}(\mathbf{k}, i\nu_n - i\omega_n)$ are the elements of (diagonal) Green's function matrix in (5). Clearly for each χ_{ij} in (8), the first term corresponds to an *intraband* contribution and the second term corresponds to an *interband* contribution. One sees that the in-plane χ_{ii} and cross χ_{ij} ($i \neq j$) have equal but opposite-sign interband contributions.

The frequency sum in (8) can easily be transformed into an integral such as (using (5))

$$\begin{aligned}
& \left[\frac{1}{\beta} \sum_{\nu_n} G_{ii}(\mathbf{k}, i\nu_n) G_{jj}(\mathbf{k}, i\nu_n - i\omega_n) \right]' \\
& = \int_{-\infty}^{\infty} \frac{dx}{2\pi} \frac{2\Gamma}{[(x - \epsilon_i)^2 + \Gamma^2][(x - \omega - \epsilon_j)^2 + \Gamma^2]} \\
& \times [f(x)(x - \omega - \epsilon_j) + f(x - \omega)(x - \epsilon_i)], \quad (9)
\end{aligned}$$

where $f(x)$ is the Fermi distribution function and we have redefined $\epsilon_1 \equiv \epsilon_+$ and $\epsilon_2 \equiv \epsilon_-$. The scattering rates are simply assumed to be identical for both bands, $\Gamma_+ = \Gamma_- \equiv \Gamma$. To obtain analytical results, we consider the two isolated layers to have the following simple band structures

$$\begin{aligned}
\xi_1(k_x, k_y) &= \frac{\hbar^2}{2m} k_{\parallel}^2 - \mu + \Delta \\
\xi_2(k_x, k_y) &= \frac{\hbar^2}{2m} k_{\parallel}^2 - \mu, \quad (10)
\end{aligned}$$

where $k_{\parallel} \equiv (k_x^2 + k_y^2)^{1/2}$ is the 2D layer momentum, μ is the chemical potential, and Δ corresponds to the energy difference between these two layer bands (in general, Δ corresponds to a *minimum* energy difference between two bands). For YBCO, we consider the CuO_2 plane as layer 1 which has generally more (hole) carriers (or less electrons) than the CuO chain which is layer 2. While the band structure (10) is oversimplified, it has captured the essential physics built in this coupled bilayer model. Taking into account the periodicity of crystals, the layer-layer coupling is chosen to be $t(k_z) = 2t_{\perp} \cos(k_z d/2)$, with the parameters t_{\perp} the coupling strength and d the spacing between two layers. When t_{\perp} is small ($|t| \ll \Delta$), one may expand $\alpha_{11} \simeq 1 - t^2/\Delta^2$, $\alpha_{22} \simeq t^2/\Delta^2$, and $\alpha_{12} \simeq |t|/\Delta$. This in turn implies that for the planar spin susceptibilities χ_{11} and χ_{22} , the intraband term is of order 1 and the interband term is proportional to t_{\perp}^2 , while χ_{12} has both intraband and interband terms proportional to t_{\perp}^2 .

With the above simplifications, the real part of the magnetic susceptibilities in (8) at zero frequency can be found to be (keeping only second order terms in t_{\perp})

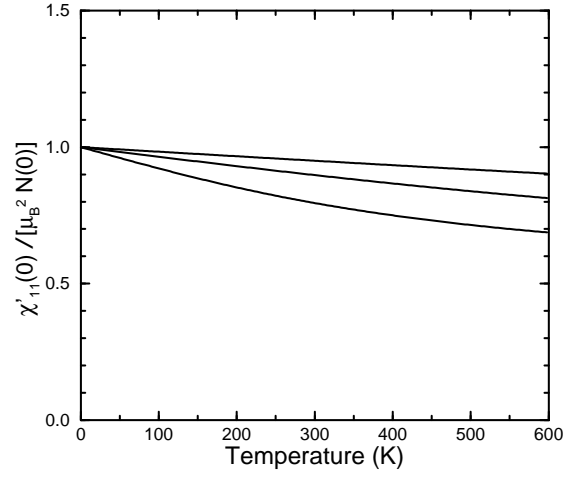


FIG. 2. Temperature dependence of the theoretical planar magnetic susceptibility $\chi'_{11}(0)$ given in (11). The curves from top to bottom correspond to $\mu = 400, 200$, and 100meV with fixed $\Delta = 20\text{meV}$, $t_{\perp} = 3\text{meV}$, and $\Gamma(T) = 20\text{meV}$ at 100K and is linear in temperature.

$$\begin{aligned}
\chi'_{11}(0) &= \mu_e^2 N(0) \left[\frac{1}{2} + \frac{1}{\pi} \arctan \left(\frac{\mu - \Delta}{\Gamma} \right) + \frac{4}{\pi} \frac{t_{\perp}^2}{\Delta^2} (\beta - \gamma) \right] \\
\chi'_{22}(0) &= \mu_e^2 N(0) \left[\frac{1}{2} + \frac{1}{\pi} \arctan \left(\frac{\mu}{\Gamma} \right) \right. \\
&\quad \left. + \frac{4}{\pi} \frac{t_{\perp}^2}{\Delta^2} \left(\frac{\mu - \Delta}{\mu} \beta - \gamma \right) \right] \\
\chi'_{12}(0) = \chi'_{21}(0) &= -\frac{2}{\pi} \frac{t_{\perp}^2}{\Delta^2} \mu_e^2 N(0) \left[\frac{2\mu - \Delta}{\mu} \beta - 2\gamma \right] \quad (11)
\end{aligned}$$

where $N(0) = m/\pi\hbar^2$ is the 2D (constant) density of states for free electron gas and we have defined

$$\begin{aligned}
\beta(T) &= \frac{\mu}{\Delta} \left[\arctan \left(\frac{\mu}{\Gamma} \right) - \arctan \left(\frac{\mu - \Delta}{\Gamma} \right) \right] \\
\gamma(T) &= \frac{\Gamma}{2\Delta} \ln \left[\frac{\mu^2 + \Gamma^2}{(\mu - \Delta)^2 + \Gamma^2} \right]. \quad (12)
\end{aligned}$$

In deriving (11), we have made use of the fact that $-\partial f(x)/\partial x \approx \delta(x)$, which is appropriate for not too high temperatures. In Fig. 2, we plot the temperature-dependent layer-1 Knight shift (proportional to $\chi'_{11}(0)$ in (11)) using the parameters which is appropriate to and has successfully described the *c*-axis optical pseudogap for underdoped $\text{YBa}_2\text{Cu}_3\text{O}_{6.6}$: $\mu = 100$ to 400meV , $\Delta = 20\text{meV}$, $t_{\perp} = 3\text{meV}$, and $\Gamma(T) = 20\text{meV}$ at 100K and is linear in temperature. It is clearly shown in Fig. 2 that the Knight shift increases only slightly as temperature decreases and does not exhibit the decreasing feature characterizing the magnetic pseudogap seen in experiments. Since in YBCO, $\Delta \ll \mu$, $\chi'_{22}(0)$ is found to be similar to $\chi'_{11}(0)$ of Fig. 2. Apart from the magnitude of t_{\perp} , it can be shown quite generally that when $\Gamma(T) < \mu$, $\beta - \gamma \sim -\Gamma^5/[\mu^3(\mu^2 + \Gamma^2)]$ which is small. This means that the last term in $\chi'_{11}(0)$ or $\chi'_{22}(0)$ in (11) does not

contribute much and one expects a similar temperature-dependent Knight shift as given in Fig. 2, even for overdoped $\text{YBa}_2\text{Cu}_3\text{O}_7$ for which t_\perp is much larger. Naively if one applies the result $\chi'_{11}(0)$ in (11) to both YBCO with smaller $\Delta = 20\text{meV}$ and LSCO with larger $\Delta \sim 0.1\text{eV}$ and assumes μ and Γ identical for both cases, one expects more significant increasing Knight shifts with decreasing temperature in overdoped LSCO compared to those in overdoped YBCO which seems consistent with experiments [28].

In contrast to the c -axis conductivity where the interband term ($\propto t_\perp^2$) dominates over the intraband term ($\propto t_\perp^4$) in the small t_\perp underdoped case, for the planar spin susceptibility, the interband term ($\propto t_\perp^2$) is almost canceled by an equal contribution arising from intraband terms. Consequently, the planar spin susceptibility is *not* very much dependent on the interband transition (or, equivalently, the magnitude of t_\perp), and, as a result, also not very dependent on temperature. Thus the Knight shift derived from the simple coupled bilayer model has only a *weak* temperature dependence mainly due to impurity scattering effect (i.e., $\Gamma(T)$).

In principle one can measure directly the effect of t_\perp with SEDOR [27]. An effective coupling a exists between spins on the two layers $a\mathbf{I}_1 \cdot \mathbf{I}_2$. In terms of our model $a \sim \hbar A^2 \chi_{12} / \mu_B^2$ where A is the hyperfine coupling constant. In order to obtain an estimate for a we take A to be the isotropic transferred hyperfine constant for Cu atoms in the CuO_2 planes of YBCO where $A/^{63}\gamma = 82\text{ kOe}$ and take $N(0) = 2\text{ states/eV-Cu}$. Evaluating χ_{12} at $T = 300\text{ K}$ with $\mu = 100\text{ meV}$ yields $\chi'_{12} / \mu_B^2 N(0) = 0.0016$. Thus the effective coupling rate is $a \simeq 15\text{ s}^{-1}$ which is about 3 orders of magnitude too small to observe experimentally [29].

While the theory given in Eq. (11) does not describe the magnetic pseudogaps for underdoped samples, several predictions and conclusions can be drawn in connection with experimental data. First, there exists a mechanism (not the interband effect) which operates most profoundly in the underdoped samples and leads to the suppression of Knight shifts (magnetic pseudogaps). Secondly, this mechanism probably contributes to the pseudogap effects seen in *all* the a - b plane measurements, including the charge-associated in-plane dc resistivity $\rho_{ab}(T)$, ARPES, in-plane scattering rate $1/\tau(\omega, T)$ in the infrared reflectivity, and the spin-associated NMR measurements and is of only secondary importance in c -axis transport. Thirdly, the interband effect we propose should dominate in the c -axis transport and is strongly associated with the pseudogap effects seen in c -axis optical and dc resistivity measurements. Fourth, as indicated in experiment on $\text{YBa}_2\text{Cu}_4\text{O}_8$ [4], the magnetic pseudogap mechanism has a much stronger effect on the CuO_2 plane (deeper normal-state Knight-shift drop) than CuO chain (weaker or almost no drop).

In summary, while at present one cannot rule out that a single mechanism may govern both the c -axis optical and a - b plane magnetic pseudogaps, we have shown through

our theoretical studies as well as with experimental data that a two-mechanism picture is favored.

The authors thank Božidar Mitrović, Tom Timusk, and Tatiana Startseva for very stimulating discussion. This work was supported by Natural Sciences and Engineering Research Council (NSERC) of Canada and Canadian Institute for Advanced Research (CIAR).

-
- [1] See, for example, Barbara Goss Levi, *Physics Today* **49**(6), 17 (1996).
 - [2] M. Takigawa, A.P. Reyes, P.C. Hammel, J.D. Thompson, R.H. Heffner, Z. Fisk, and C. Ott, *Phys. Rev. B* **43**, 247 (1991).
 - [3] R.E. Walstedt, R.F. Bell, L.F. Schneemeyer, J.V. Waszczak, and G.P. Espinosa, *Phys. Rev. B* **45**, 8074 (1992).
 - [4] M. Bankay, M. Mali, J. Roos, and D. Brinkmann, *Phys. Rev. B* **50**, 6416 (1994).
 - [5] R. Stern, M. Mali, I. Mangelschots, J. Roos, D. Brinkmann, J.-Y. Genoud, T. Graf, and J. Muller, *Phys. Rev. B* **50**, 426 (1994).
 - [6] Ya-Wei Hsueh, B. W. Statt, M. Reedyk, J. S. Xue, and J. E. Greedan, *Phys. Rev. B*, submitted.
 - [7] A. J. Millis, H. Monien, and D. Pines, *Phys. Rev. B* **42**, 167 (1990).
 - [8] H. Monien, D. Pines, and M. Takigawa, *Phys. Rev. B* **43**, 258 (1991).
 - [9] A.V. Chubukov, D. Pines, and B.P. Stojković, preprint.
 - [10] V. J. Emery and S. A. Kivelson, *Nature* **374**, 434 (1995).
 - [11] K. Takenaka, K. Mizuhashi, H. Takagi, and S. Uchida, *Phys. Rev. B* **50**, 6534 (1994).
 - [12] C. C. Homes, T. Timusk, R. Liang, D. A. Bonn, and W. N. Hardy, *Phys. Rev. Lett.* **71**, 1645 (1993).
 - [13] C. C. Homes, T. Timusk, D. A. Bonn, R. Liang, and W. N. Hardy, *Physica C* **254**, 265 (1995).
 - [14] D. N. Basov, R. Liang, B. Dabrowski, D.A. Bonn, W.N. Hardy, and T. Timusk, *Phys. Rev. Lett.* **77**, 4090 (1996).
 - [15] M. Reedyk, T. Timusk, Y.-W. Hsueh, B.W. Statt, J. S. Xue, and J. E. Greedan, preprint.
 - [16] G.V.M. Williams, J.L. Tallon, E.M. Haines, R. Michalak, and R. Dupree, *Phys. Rev. Lett.* **78**, 721 (1997).
 - [17] See, for example, A. G. Loeser *et al.*, *Science* **273**, 325 (1996).
 - [18] W. A. Atkinson and J. P. Carbotte, *Phys. Rev. B* **55**, 3230 (1997).
 - [19] W. A. Atkinson, W. C. Wu, and J. P. Carbotte, *Phys. Rev. Lett.*, submitted.
 - [20] W. C. Wu, W. A. Atkinson, and J. P. Carbotte, *Phys. Rev. B*, submitted.
 - [21] Y. Zha, S. L. Cooper, and D. Pines, *Phys. Rev. B* **53**, 8253 (1996).
 - [22] D. N. Basov, H.A. Mook, B. Dabrowski, and T. Timusk, *Phys. Rev. B* **52**, R13141 (1995).
 - [23] S. Uchida, K. Tamasaku, and S. Tajima, *Phys. Rev. B* **53**, 14558 (1996).

- [24] G. Boebinger *et al.*, Phys. Rev. Lett. **77**, 5417 (1996).
- [25] T. Startseva *et al.*, preprint.
- [26] See, for example, S. Doniach and E.H. Sondheimer, *Green's Functions for Solid State Physicists* (W.A. Benjamin, Reading, Massachusetts, 1974), p. 162.
- [27] C. Slichter, *Principles of Magnetic Resonance*, 3rd ed. (Springer-Verlag, New York, 1990).
- [28] T. Nakano, M. Oda, C. Manabe, N. Momono, Y. Miura, and M. Ido, Phys. Rev. B **49**, 16000 (1994).
- [29] B.W. Statt, L.M. Song, and C.E. Bird, Phys. Rev. B, May 1997 issue.